INORGANIC CHEMISTRY

FRONTIERS

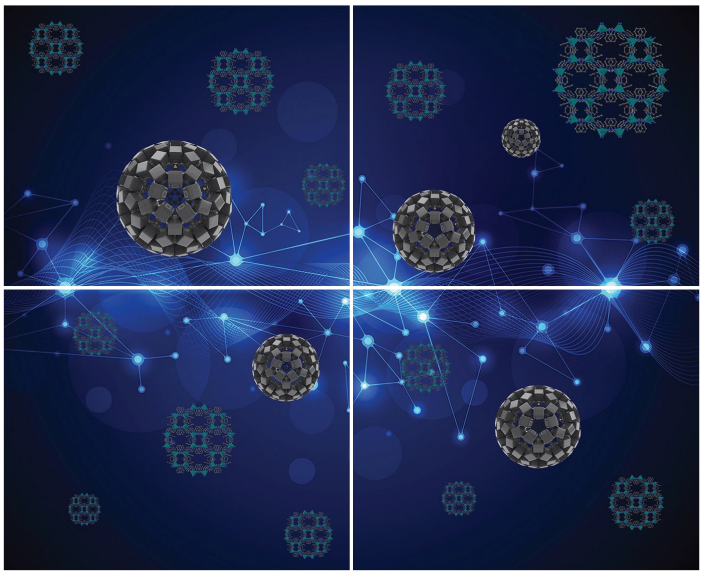

Accepted Manuscript

This article can be cited before page numbers have been issued, to do this please use: L. Huang, J. Fidelius, K. Schwedtmann, P. Royla, R. M. Gomila, A. Frontera and J. J. Weigand, *Inorg. Chem. Front.*, 2026, DOI: 10.1039/D6QI01242F.

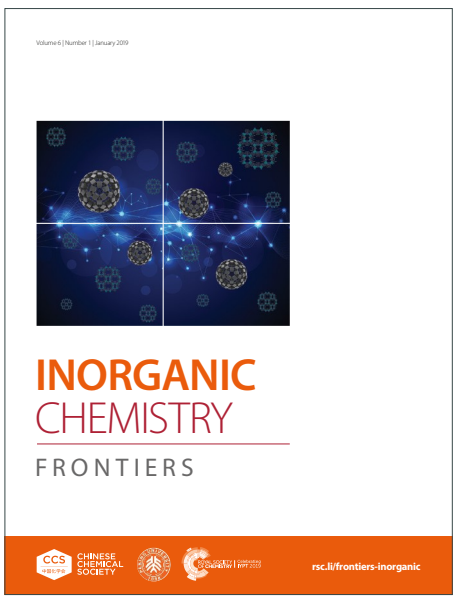

View Article Online
DOI: 10.1039/D6QI01242F

ARTICLE

Three-Component Diazaphospholium Synthesis Enables P(V)-to-P(III) Conversion and Ylide-Mediated CO_2 and CS_2 Activation

Linwei Huang,[a] Jannis Fidelius,[a] Kai Schwedtmann,[a] Philipp Royla,[a] Rosa M. Gomila,[b] Antonio Frontera,[b] and Jan J. Weigand*[a]

Received 00th January 20xx,
Accepted 00th January 20xx

DOI: 10.1039/x0xx00000x

Diazaphospholium triflate salts **3**[OTf]$_2$ were synthesized through a three-component (1+2+2)-cycloaddition of the imidazoliumyl-subsituted phosphenium surrogate [$\mathbf{L_C}$-P(OTf)Ph]$^+$ cation ($\mathbf{L_C}$ = 4,5-dimethyl-1,3-diisopropylimidazolium) with nitriles and *N*-benzylideneaniline. These P(V) heterocycles display pronounced base-dependent reactivity. Treatment with 4-dimethylaminopyridine (DMAP) triggers a 1,2-phenyl migration and a formal P(V)-to-P(III) conversion, affording cationic DMAP adducts that can be further transformed into azaphospholes bearing P–O, P–C, and P–N bonds. Key intermediates and products were isolated and fully characterized, and the proposed mechanism is supported by DFT calculations. In contrast, reaction of diazaphospholium triflate **3**[OTf]$_2$ with 1,8-diazabicyclo[5.4.0]undec-7-ene (DBU), followed by deprotonation, furnishes an ylide featuring a directional, strong N···P interaction. This species exhibits not only classical *Wittig*-type reactivity but also unusual CO_2 and CS_2 activation, leading to oxazinedione- or thiazinedithione-type products alongside the corresponding phosphole chalcogenides.

Introduction

Phosphorus-containing heterocycles have garnered significant attention owing to their widespread applications in pharmaceutical agents,[1,2] materials,[3,4] and organic synthesis.[5,6] Among the reported synthetic methodologies for these compounds, condensation and cycloaddition reactions are the two most commonly employed protocols. The former typically employs simple or pre-designed phosphorus building blocks to construct more complex molecules and requires careful consideration of functional group tolerance during the process. In contrast, cycloaddition reactions form cyclic products through efficient processes and have therefore attracted considerable attention.[7] A representative example is the (3+2)-cycloaddition reaction of phosphaalkynes with azides, which provides efficient access to 1,2,3,4-triazaphospholes,[8–11] albeit being constrained to highly reactive phosphaalkynes.

Phosphenium ions [R_2P]$^+$ are dicoordinate phosphorus species featuring six-valence electrons, rendering them isoelectronic with neutral carbenes. Considerable efforts have been devoted to stabilizing these highly reactive species through electronic and steric effects imposed by substituents (R = *e.g.* amino, alkyl, aryl, cyclopentadienyl, ferrocenyl).[12–38] Owing to their high electrophilicity, they have long served as versatile synthons for constructing phosphorus-containing frameworks. They readily engage in insertion and addition reactions (*e.g.* (1,4)- and (2,4)-additions) with unsaturated substrates to form diverse phosphorus-containing compounds.[12,17,39,40]

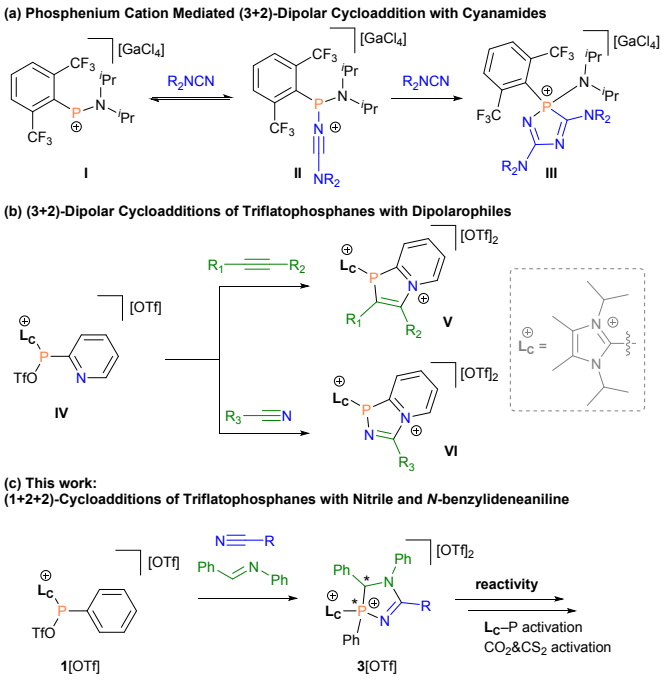

Figure 1 (**a**) Dipolar (3+2) cycloaddition of a phosphenium–cyanamide acid–base adduct **II** with a second equivalent of cyanamide, affording a cationic five-membered heterocycle **III**; R = Me, ^{i}Pr. (**b**) Two-component (3+2)-cycloaddition of an imidazoliumyl-substituted triflatophosphane **IV** with alkynes and nitriles to access azaphospholium salts **V** and **VI**; R_1 = H, R_2 = aromatic groups, or R_1 = R_2 = aromatic groups; R_3 = alkyl or aromatic groups. (**c**) This work: three-component (1+2+2)-cycloaddition of **1**[OTf] with nitriles and a *N*-benzylideneaniline to access diazaphospholium salts **3**[OTf]$_2$; R = aromatic groups. Stereocenters are marked by asterisk [*].

[a] *Faculty of Chemistry and Food Chemistry, Technische Universitat Dresden, 01062 Dresden, Germany. E-mail: jan.weigand@tu-dresden.*
[b] *Department of Chemistry, Universitat de Illes Balears, 07122 Palma de Mallorca, Spain.*

View Article Online
DOI: 10.1039/D6QI01242E

In 2002, Bertrand and co-workers reported a (3+2)-dipolar cycloaddition of phosphenium cation **I** with cyanamides to give adducts of type **II**, which react with a second equivalent of cyanamide, affording cationic five-membered heterocycles **III** (**Figure 1a**).[41]

Recently, our group reported the imidazoliumyl-substituted phosphenium surrogate **IV**, which activates dipolarophiles such as alkynes and nitriles to access a range of azaphospholium salts **V** and **VI** *via* a (3+2)-cycloaddition route (**Figure 1b**).[42,43] Inspired by these results, we envisioned that the phosphenium surrogate **1**[OTf] could promote a (1+2+2)-cycloaddition, thus granting access to azaphospholium architectures (**Figure 1c**). Moreover, the imidazoliumyl group should enable post-modification *via* L_C–P bond activation, *e.g.* through processes in which the L_C-substituent acts as a leaving group liberating the free NHC upon reduction or substitution reactions with a Grignard reagent.[44]

Despite their rich chemistry in these two-component reactions, the utility of phosphenium cations in multicomponent cycloaddition reactions remains largely unexplored. Herein, we report a three-component reaction of the imidazoliumyl-substituted phosphane **1**[OTf] with nitriles and an *N*-benzylideneaniline to afford a series of five-membered diazaphospholium triflate salts **3**[OTf]$_2$. The L_C–P bond in these products can be selectively engaged by the choice of bases, resulting in divergent downstream reactivity. Treatment of **3a-c**[OTf]$_2$ with 4-dimethylaminopyridine (DMAP) promotes either 1,2-phenyl migration or ring opening, leading in both cases to a rare formal P(V)-to-P(III) conversion, as supported by DFT calculations and the full characterization of intermediates and products. Further functionalization of the resulting adduct **5a**[OTf] provides access to a range of azaphospholes. In contrast, treatment of **3a**[OTf]$_2$ with 1,8-diazabicyclo[5.4.0]undec-7-ene (DBU) affords a phosphorus ylide that exhibits *Wittig*-type reactivity. This ylide further reacts with aldehydes, CO_2, and CS_2, most likely *via* a distinctive bimolecular pathway, to give a series of DBU-derived products.

Results and discussion

Synthesis

The triflato-phosphane **1**[OTf] was prepared analogously to literature procedures *via* chloride abstraction from the chlorophosphane precursor using AgOTf.[12,45] It displays a downfield-shifted resonance in the ^{31}P NMR spectrum [$\delta(^{31}P)$ = 113.5 ppm], within the range reported for structurally characterized triflato-phosphanes.[42,43] To probe the electrophilic behavior of the P atom in **1**[OTf], we screened its reaction with various nitriles. Treating **1**[OTf] with benzonitrile or 4-methoxybenzonitrile at 80 °C for 16 hours resulted in no observable reaction. In contrast, use of the more nucleophilic 4-(dimethylamino)benzonitrile afforded the cycloaddition product **2**[OTf]$_2$ in near quantitative yield (96%). Suitable crystals for single-crystal X-ray diffraction (scXRD) analysis confirmed the molecular structure (**Figure 2a**). This result is reminiscent of the previously reported trapping of electrophilic phosphorus cations by strongly donating nitriles to furnish cationic five-membered heterocycles.[46] Although no discrete 1^+–nitrile adduct was isolated, the formation of **2**[OTf]$_2$ and its structural metrics are consistent with initial nitrile coordination to cation 1^+ as the entry point to cycloaddition.

Motivated by this, we investigated a strategy to engage less nucleophilic nitriles by introducing a second, complementary two-atom component. *N*-benzylideneaniline was found to be a suitable substrate for this three-component conversion and the synthetic route is outlined in **Scheme 1**. Treatment of stoichiometric amounts of benzonitrile, *N*-benzylideneaniline, and **1**[OTf] in DCM at 80 °C for 12 h in a pressure-sealed tube afforded the desired product **3a**[OTf]$_2$. The product was recrystallized from CH_2Cl_2/Et_2O and isolated in 84% yield on a 10 gram scale. The ^{31}P NMR spectrum of **3a**[OTf]$_2$ revealed two resonances at $\delta(^{31}P)$ = 55.0 ppm [*syn*-(S_P, R_C), 93%] and $\delta(^{31}P)$ = 60.2 ppm [*anti*-(S_P, S_C), 7%], corresponding to two diastereomeric configurations and in agreement with a larger characteristic $^2J_{HP}$ coupling constant of 11 Hz observed in the ^{1}H NMR spectrum for *syn*-**3a**[OTf]$_2$.[47] These assignments were unambiguously confirmed by scXRD analysis of triflate salts of both diastereomers (see the **SI**, **Figure S106**). The two diastereomers of cations **3a-c**$^{2+}$ arise from the stereogenic carbon atom in the *N*-benzylideneaniline and the phosphorus atom upon cycloaddition.[48]

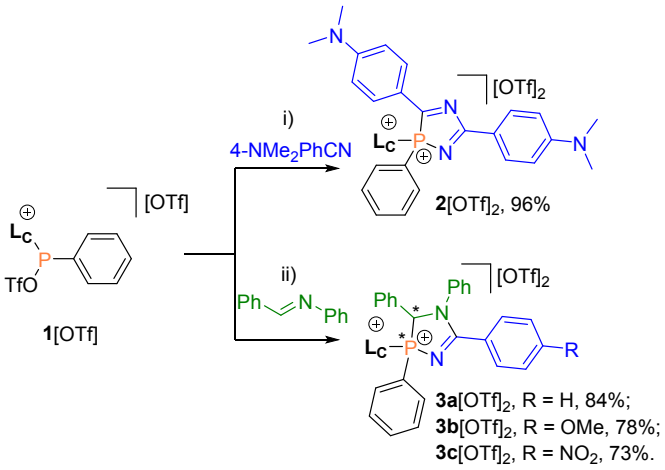

Scheme 1 Synthesis of diazaphospholium salts **2**[OTf]$_2$ and **3a-c**[OTf]$_2$. i) 2 equiv. 4-(dimethylamino)benzonitrile, DCM, r.t., 30 min, 96%. ii) 1 equiv. **1**[OTf], 1 equiv. benzonitrile derivative, and 1 equiv. *N*-benzylideneaniline, DCM, 80 °C (pressure sealed tube), 12 h, 84% (for **3a**[OTf]$_2$), 78% (for **3b**[OTf]$_2$) and 73% (for **3c**[OTf]$_2$). Stereocenters are marked by asterisk [*].

This reaction tolerates both electron-donating and electron-withdrawing substituents, such as 4-methoxy- and 4-nitrobenzonitrile, affording **3b,c**[OTf]$_2$ in good yields (78 and 73%). The molecular structures of **3a,b**[OTf]$_2$ were verified by scXRD analysis (see *anti*-**3a**[OTf]$_2$,**Figure 2b** and *anti*-**3b**[OTf]$_2$ in the **SI**, **Figure S21**). The observed P–C bond lengths in **3a**$^{2+}$ [P1–C1 1.8160(14) Å, P1–C2 1.7682(15) Å] fall within the typical single bond range for azaphospholium salts.[46] The P1–N1 single bonds in azaphospholium cations **3a,b**$^{2+}$ [**3a**$^{2+}$, 1.6312(12) Å; **3b**$^{2+}$, 1.625(2) Å] are comparable to that of **2**$^{2+}$ [1.615(3) Å],

View Article Online
DOI: 10.1039/D6QI01242F

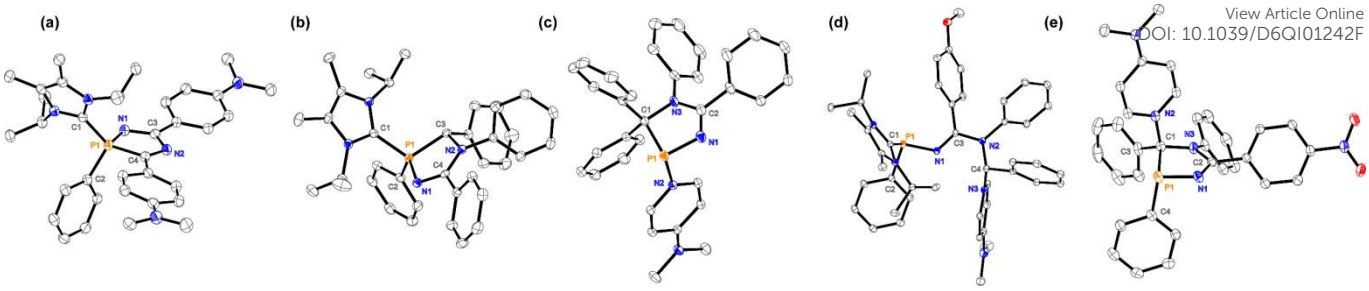

Figure 2 Molecular structures of $\mathbf{2}^{2+}$ in **2**[OTf]$_2$ (**a**), *anti*-**3a**$^{2+}$ in *anti*-**3a**[OTf]$_2$ (**b**), **5a**$^+$ in **5a**[OTf] · 0.5 CH_2Cl_2 (**c**), $\mathbf{6}^{2+}$ in **6**[OTf]$_2$· 0.666 CH_2Cl_2 (**d**) and *anti*-**4**$^+$ in *anti*-**4**[OTf] (**e**); hydrogen atoms, anions, and solvent molecules are omitted for clarity; thermal ellipsoids are displayed at 50% probability (100 K); selected bond lengths (in Å) and angles (in °): **2**[OTf]$_2$, P1–C1 1.819(3), P1–C2 1.793(3), P1–N1 1.615(3); *anti*-**3a**[OTf]$_2$, P1–C1 1.8160(14), P1–C2 1.7682(15), P1–N1 1.6312(12); **5a**[OTf], P1–C1 1.9338(12), P1–N1 1.6862(10), P1–N2 1.7840(9); **6**[OTf]$_2$, P1–C1 1.835(4), P1–C2 1.830(4), P1–N1 1.702(3); *anti*-**4**[OTf], P1–C1 1.942(3), P1–C2 1.831(3), C1–N2 1.521(3), P1–N1 1.711(2).

further indicating that the cycloaddition involves interaction of the electrophilic phosphorus with the cyano group.

Phosphonium salts containing an α-C–H bond readily undergo deprotonation and have been exploited in *Wittig* reactions.[49–51] Given their structural similarity to such phosphonium salts, these azaphospholium salts are anticipated to exhibit related reactivity. At the same time, the **L$_C$**–P bond is base-sensitive, which potentially enables its functionalization. Accordingly, the deprotonation of these cyclic azaphospholium salts **3a-c**[OTf]$_2$ was evaluated. However, treatment with ionic bases, such as potassium bis(trimethylsilyl)amide (KHMDS) or potassium *tert*-butoxide (KO^{t}Bu) led to unselective conversions in all cases. In contrast, reactions with neutral N-bases such as DMAP or DBU yielded well-defined and isolable species.

Addition of DMAP to a suspension of **3a**[OTf]$_2$ in C_6H_5F or THF gave a yellow solution within 2 hours at room temperature. ^{31}P NMR spectroscopic analysis of aliquots removed from the reaction mixture revealed two distinct resonances at $\delta(^{31}P) = 98.0$ and 112.3 ppm, and the ^{1}H NMR spectrum confirmed the formation of [**Lc**–H][OTf] (see the **SI**, Section **S4.1**).

Reactions with nitrogen base DMAP

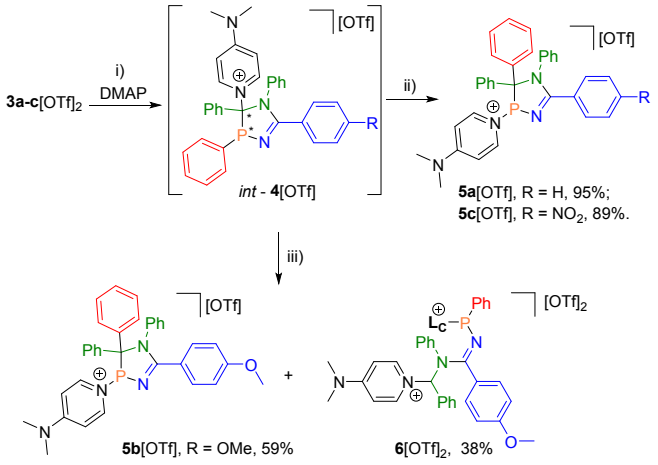

Scheme 2 Reactions of **3a**-**c**[OTf]$_2$ with DMAP. i) + DMAP, - [**L$_C$**-H][OTf], C_6H_5F or THF, r.t., 2 h, 89% (for **4**[OTf]). ii) Rearrangement to **5a**,**b**[OTf] (r.t., 12 h), 95% (for **5a**[OTf]), 59% (for **5b**[OTf]) or to **5c**[OTf] (r.t., 7 days; or dissolution in DCM, overnight), 89%. iii) Competing C–P bond cleavage observed predominantly for **3b**[OTf]$_2$, affording **6**[OTf]$_2$, 38%. Stereocenters are marked by asterisk [*].

Repeated ^{31}P NMR spectroscopic analysis after another 16 hours at room temperature revealed the complete consumption of both resonances in favor of a new resonance at $\delta(^{31}P) = 141.4$ ppm, which was unambiguously identified as **5a**[OTf] by scXRD (**Figure 2c**). The P–N bond length in **5a**$^+$ (P1–N2 1.7840(9) Å) is consistent with that of the known N–P(III) acid-base adduct (*e.g.* DMAP–PPh_2: 1.789(1) Å]).[52]

In an effort to rationalize this reactivity and identify the observed intermediates, conversions of **3b**[OTf]$_2$ and **3c**[OTf]$_2$ with DMAP were conducted under identical conditions. The reaction of **3b**[OTf]$_2$ afforded two main products that were isolated, fully characterized, and identified as **5b**[OTf] (see the **SI**, **Figure S40**) and **6**[OTf]$_2$ (**Figure 2d**) by scXRD, respectively. The product **6**[OTf]$_2$ is consistent with C–P bond scission following nucleophilic addition of DMAP; its connectivity was established by multinuclear NMR spectroscopy. In contrast, treatment of **3c**[OTf]$_2$ led to a brown suspension after 3 days, and ^{31}P NMR analysis of the mixture by dissolution in DCM revealed resonances at $\delta(^{31}P) = 100.6$ and 110.8 ppm, consistent with those observed for **3a**[OTf]$_2$ under analogous conditions. Recrystallization of the crude solid from DCM/Et_2O allowed identification of diastereomeric **4**[OTf] (**Figure 2e**), featuring two stereogenic centers. Prolonged reaction times (> 1 week) or dissolution of **4**[OTf] in DCM overnight resulted in exclusive formation of **5c**[OTf]. Taken together, these results are consistent with DMAP attack at the internal α-carbon to give a pyridinium-type intermediate (**4**$^+$). From this branch point, two competing pathways are operative: (i) departure of the **L$_C$** group to either furnish isolable **4**[OTf] or trigger 1,2-phenyl migration to give **5**[OTf], or (ii) C–P bond scission to give the ring-opened product **6**[OTf]$_2$ (predominantly for R = OMe). Notably, the nitro-substituted intermediate **4**[OTf] is sufficiently stabilized to be isolated.

To corroborate our experimental findings, we performed DFT calculations at the BP86-D4/def2-TZVP level of theory (COSMO = C_6H_5F) and propose the mechanism outlined in **Figure 3**, which involves four transition states (**TS**) and three intermediates (**INT**) that are consistent with experimental observations of transient species by *in situ* NMR spectroscopy.

View Article Online
DOI: 10.1039/D6QI01242F

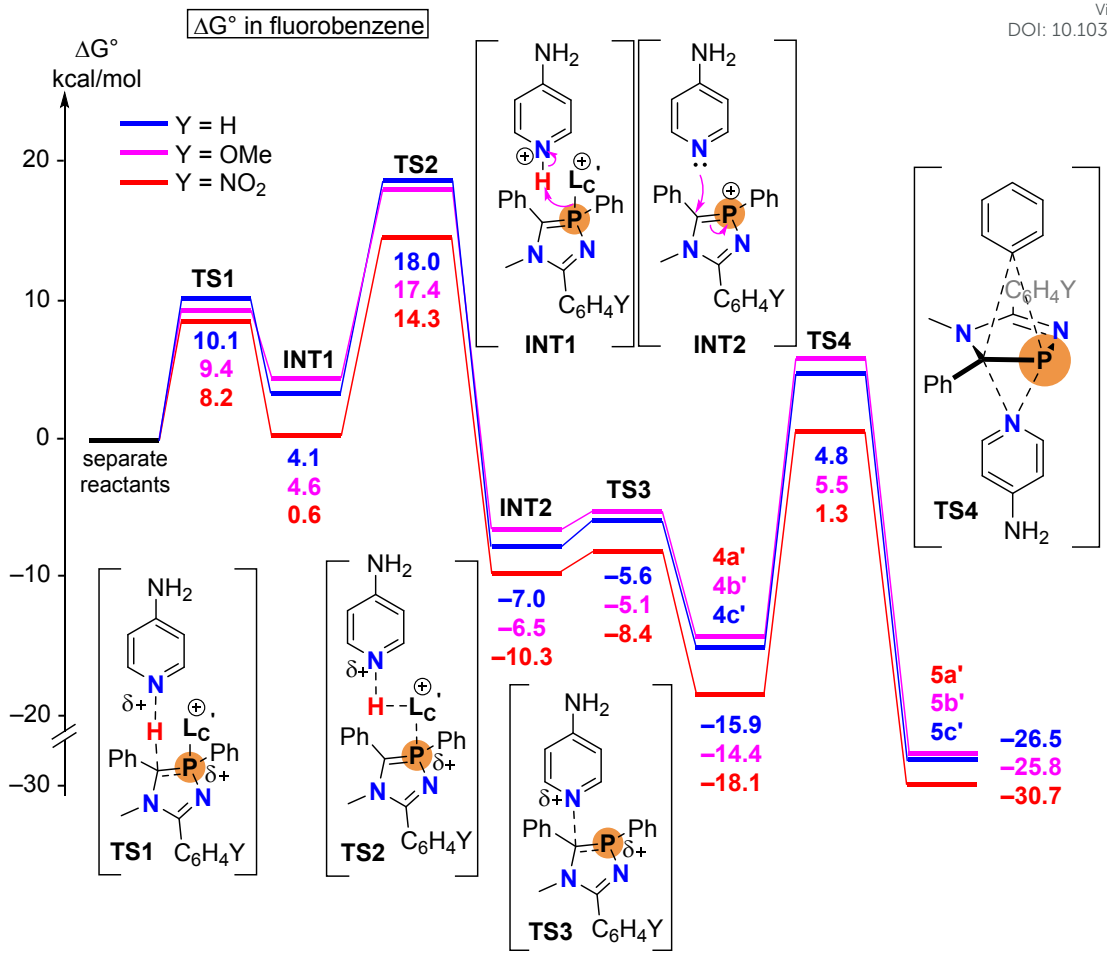

Figure 3 Reaction profile (ΔG° in kcal/mol) for the transformation process, at the BP86-D4/def2-TZVP level of theory (COSMO = C_6H_5F). The reactants were simplified as **3a'-c'**. Specifically, the phenyl group attached to the nitrogen atom of N-benzylideneaniline was replaced with a methyl group, as this group is not involved in the mechanistic steps. DMAP was replaced by 4-aminopyridine (**AP**), and the $\mathbf{L_C}$ substituent was simplified as 1,3-dimethylimidazolium (denoted as $\mathbf{L_C'}$). Y = H, $[\mathbf{3a}]^{2+}$; OMe, $[\mathbf{3b}]^{2+}$; NO_2, $[\mathbf{3c}]^{2+}$.

For computational efficiency, all structures were optimized on simplified models (see caption of **Figure 3**). The mechanism proceeds through several key steps. The initial step involves the abstraction of an acidic proton adjacent to the phosphorus atom by 4-aminopyridine (**AP**), leading to the formation of the first intermediate (**INT1**). Subsequently, **INT1** converts to the second intermediate (**INT2**) *via* elimination of $[\mathbf{L_C'}–H]^+$. In this process, **AP** acts as an acid-base catalyst, facilitating this elimination. The next step is a nucleophilic attack, in which a second **AP** molecule acts as a nucleophile, attacking the deprotonated carbon atom of the C=P$^+$(Ph)N group (**INT2**). This forms the intermediates **4a'-c'**, depending on the Y-substituent. Finally, a 1,2-phenyl shift yields the final products **5a'-c'** in a concerted manner, as further discussed below.

The reaction profile provides the following energetic insights (Gibbs energies in kcal/mol). The first transition step, proton abstraction, presents a low activation barrier, ranging from 8.2 kcal/mol (for Y = NO_2) to 10.1 kcal/mol (for Y = H). It is endergonic for all substituents, with Y = OMe being the least stable (4.6 kcal/mol). Notably, for Y = OMe, the reverse reaction barrier is very small (4.8 kcal/mol). Therefore, in this case, the concentration of **INT1** is very low compared to the starting material, which rationalizes an increased susceptibility toward competing nucleophilic pathways under these conditions (including C–P bond scission), although the ring-opening pathway itself was not explicitly modelled computationally. Further support for this interpretation is the lower positive charge at the H-atom in **3b'** compared to **3a'** and **3c'**, suggesting lower acidity and allowing the competitive nucleophilic attack (**Table 1**).

Table 1 Charges in [*e*] for the H atom α to the P-atom in **3a'-c'** using different methods

Method	3a'	3b'	3c'
Mulliken	0.1764	0.1755	0.1780
NPA	0.2543	0.2497	0.2566
MK	0.1339	0.1281	0.1422
Löwdin	0.1650	0.1635	0.1660

The subsequent step, elimination of $[\mathbf{L_C'}–H]^+$, is identified as the turnover-limiting event within the computed free-energy profiles, leading to the second intermediate. This step is exergonic and irreversible, with step barriers of 13-14 kcal/mol. The overall barrier energies are higher for Y = H and OMe (18.0 and 17.4 kcal/mol, respectively) compared to Y = NO_2

(14.3 kcal/mol). The nucleophilic attack by **AP** exhibits a very low activation barrier (1-2 kcal/mol), yielding compounds **4a'**-**c'**. This step is also exergonic, with the nitro derivative (Y = NO_2) showing significant additional stabilization, which aligns well with the experimental observation that compound **4**[OTf] is the only isolable intermediate. The final 1,2-phenyl shift is exergonic. Notably, while this step can display a comparatively large intrinsic barrier relative to its preceding minimum, the preceding intermediate is substantially stabilized such that the corresponding transition state lies only slightly above the starting materials on the overall profile.

The optimized geometries of **TS1**-**TS4** for Y = H were used as representative models for the series and are shown in the **SI**, together with the Cartesian coordinates for all computed structures. Standard bond-forming and bond-breaking distances are observed for **TS1** and **TS3**. **TS4**, which corresponds to the 1,2-phenyl shift, represents a concerted but asynchronous process, indicating that the intermediate and final product are connected by a single transition state. For all three systems studied, the **AP** ring initiates the rearrangement first, followed by the subsequent migration of the phenyl ring. In the transition state, the phenyl ring is almost equidistant from the carbon and phosphorus atoms, while the **AP** ring is considerably closer to the phosphorus atom.

Functionalization of 5[OTf]

As reported previously by our group, the P(III) reagent, $(DMAP)_3P[OTf]_3$ has served as a versatile electrophilic P(III) synthon for constructing a variety of P-functionalized compounds.[53] Likewise, **5a**[OTf] proved amenable to further functionalization by acting as an electrophilic azaphosphole-type P(III) fragment transfer reagent. Accordingly, reaction of **5a**[OTf] with PhMgBr, PhOH (in the presence of Et_3N), and $KNPh_2$ furnished the P–C-, P–O-, and P–N-functionalized azaphosphole derivatives **7**, **8**, and **9**, respectively (**Scheme 3**), which were isolated as analytically pure solids and fully characterized (see the **SI** for details; including scXRD for **7**-**9**).

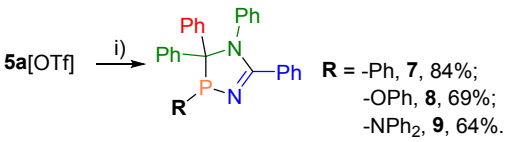

Scheme 3 Functionalization reactions of **5a**[OTf]; i) for **7**, + PhMgBr, - DMAP, - MgBrOTf, r.t., 2 h, 84%; for **8**, + PhOH, + Et_3N, - DMAP, - Et_3N-HOTf, 60 °C, 2 h, 69%; for **9**, + $KNPh_2$, - KOTf, - DMAP, r.t., 2 h, 64%.

Compared to the parent azaphosphole framework, the ^{31}P NMR resonances of these products are shifted upfield ($\delta(^{31}P)$ = 98.1 ppm (**7**), 108.4 ppm (**8**), and 147.5 ppm (**9**)), consistent with substitution at the tricoordinate phosphorus center.[54] Overall, this methodology provides straightforward access to structurally elaborate cyclic phosphorus compounds that are difficult to obtain by conventional approaches. The coordination and catalytic applications of these azaphospholes are under investigation in our group.

Reactions with nitrogen base DBU

The aforementioned results suggest that the basicity and nucleophilicity of the base significantly influence the activation pathway. To further probe this effect, other bases were examined in reactions with diazaphospholium compounds **3a**-**c**$[OTf]_2$. The reaction with 1,5-diazabicyclo[4.3.0]non-5-ene (DBN) afforded non-separable mixtures in all cases (**Figure S112-113**). In contrast, treatment of **3a**$[OTf]_2$ with one equivalent of 1,8-diazabicyclo[5.4.0]undec-7-ene (DBU) in THF at room temperature gave a yellow suspension within 2 hours. Analysis of the supernatant by ^1H NMR spectroscopy confirmed the formation of [L_C–H][OTf], whereas a solution of the precipitate (**10**[OTf]) in CD_2Cl_2 exhibited two resonances at $\delta(^{31}P)$ = 23.4 and 18.0 ppm (6:1 integral ratio) in the ^{31}P NMR spectrum, assigned to *syn*- and *anti*-diastereomers of **10**[OTf] (**Scheme 4, I**). Single crystals suitable for scXRD analysis were obtained by diffusion of Et_2O into a saturated DCM solution, and the molecular structure of *syn*-**10**$^+$ is shown in **Figure 4a**. Contrary to expectation, functionalization of DBU with the azaphosphole fragment occurs *via* C–P over N–P bond formation, which has been previously observed in phosphorylation reactions of DBU.[55,56] Notably, the P1–N1 atom distance (2.306 Å) is longer than the single-bond length (P–N 1.82 Å),[57] yet shorter than the sum of the Van der Waals radii (3.35 Å),[58] indicating a possible intramolecular interaction. The P1–C1 bond length (1.836 Å) aligns with a typical P–C single bond.

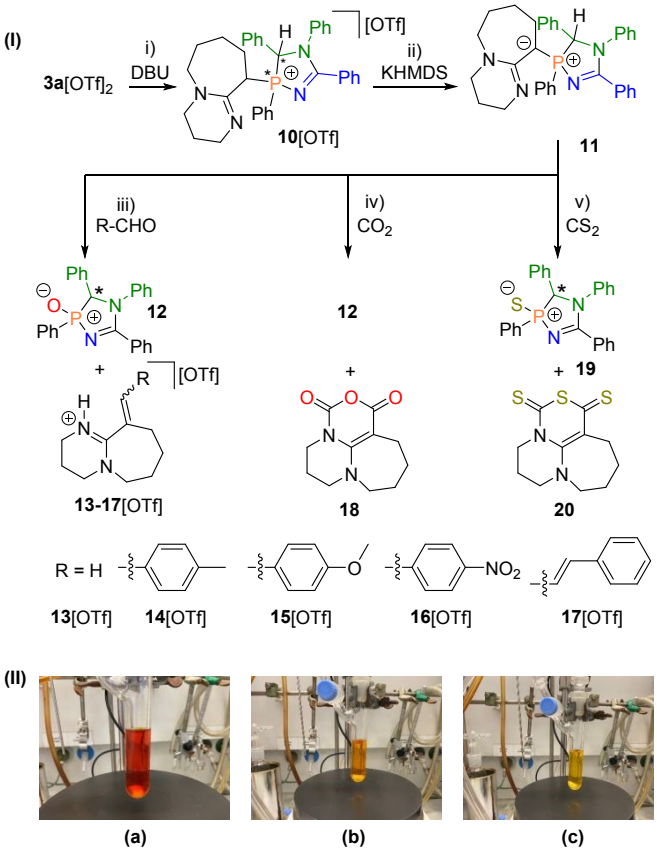

Scheme 4 (**I**) i) + DBU, - [L_C-H][OTf], THF, r.t., 2-12 h, 78%. ii) + KHMDS, - HMDS, - KOTf, THF, r.t., 2 h, 86%. iii) THF, r.t., 2-12 h or 60 °C, 2 h. Paraformaldehyde, **13**[OTf], 74%; 4-

View Article Online
DOI: 10.1039/D6QI01242F

MeOPhCHO, *E*-**14**[OTf], 64%; 4-MePhCHO, *E*-**15**[OTf], 76%; 4-NO_2PhCHO, *Z*-**16**[OTf], 60%; *E*-Cinnamaldehyde, *Z*,*E*-**17**[OTf], 78%. iv) 2 bar CO_2, -196 °C to r.t., C_6D_6, 10 min or 1 bar CO_2, r.t., THF, 10-30 min, 71%; v) CS_2, THF, r.t., 10 min, 52%. (**II**) Photographic representation of CO_2 activation by **11** in THF under a CO_2 atmosphere (1 atm) at room temperature. The THF solution of **11** before exposure to CO_2 (**a**), after exposure to CO_2 for 10 min (**b**), and after exposure to CO_2 for 20 min (**c**). Stereocenters are marked by asterisk [*].

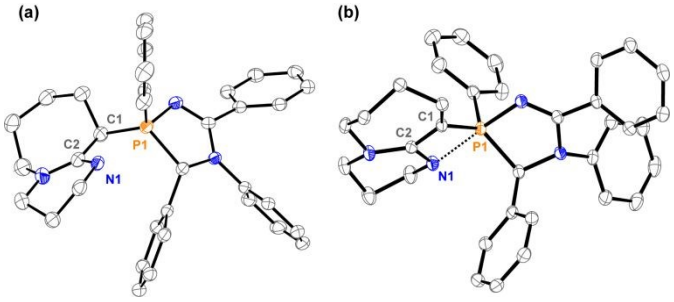

Figure 4 Molecular structures of *syn*-**10**$^+$ in *syn*-**10**[OTf] (**a**) and **11** (**b**); hydrogen atoms and other solvent molecules are omitted for clarity; thermal ellipsoids are displayed at 50% probability (100 K); selected bond lengths (in Å) and angles (in °): **10**[OTf]: P1–C1 1.836(3), C1–C2 1.490(5), C2–N1 1.298(5), P1–C1–C2 98.8(2), C1–C2–N1 110.5(3); **11**: P1–C1 1.7488(12), C1–C2 1.3987(17), C2–N1 1.3652(17), P1–N1 1.9670(11), C1–P1–N1 72.39(5), P1–C1–C2 94.47(8), C1–C2–N1 105.58(10), C2–N1–P1 86.41(8).

Reactions of **3b**[OTf]$_2$ and **3c**[OTf]$_2$ with DBU gave complex mixtures. These observations are well supported by the computed electronic properties of the systems. The decreased α-proton acidity in **3b** redirects the pathway toward unselective nucleophilic side-reactions, whereas the strong stabilization of intermediates induced by the nitro group in **3c** increases the effective kinetic barriers for the subsequent steps, leading in both cases to the observed complex mixtures.

The mechanism for the transformation of **3a**' to **10**' was investigated using DFT calculations, and the proposed pathway is illustrated in **Figure 5**. The mechanism begins with a proton abstraction similar to that described above for DMAP. Specifically, the nitrogen atom of DBU abstracts the proton adjacent to the positively charged phosphorus atom *via* **TS1**. This step exhibits a low activation energy and is exergonic by 7.8 kcal/mol. Subsequently, **L$_C$**$^+$ abstracts a proton from the seven membered ring, which is activated and sufficiently acidic due to the adjacent iminium group. This proton transfer constitutes the rate determining step of the reaction, possessing a global activation barrier of 23.3 kcal/mol. This process generates an enamine intermediate along with the formation of [**L$_C$**'–H]$^+$. Finally, the nucleophilic enamine attacks the phosphorus atom (**TS3**) with a concurrent proton transfer, yielding the final product **10**. This final step has a low activation energy, with **TS3** located only 3.0 kcal/mol above the starting materials. Moreover, the formation of **10** is highly exergonic by –10.1 kcal/mol, providing strong thermodynamic support for its formation.

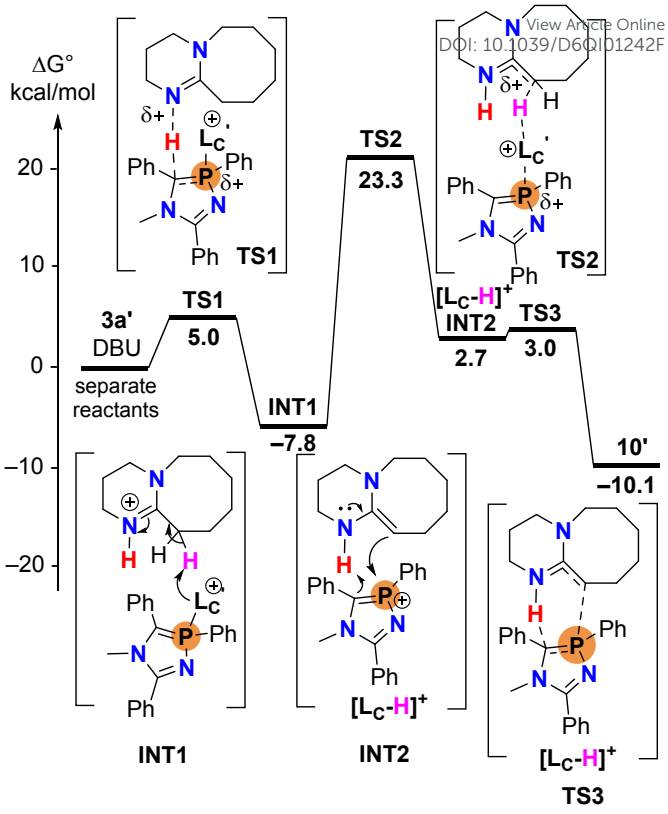

Figure 5 Reaction profile (ΔG° in kcal/mol) for the transformation process, at the BP86-D4/def2-TZVP level of theory. The reactant was simplified as **3a'**. Specifically, the phenyl group attached to the nitrogen atom of N-benzylideneaniline was replaced with a methyl group, as this group is not involved in the mechanistic steps.

Small molecules activation

Deprotonation of the phosphonium salt **10**[OTf] with KHMDS readily formed the corresponding ylide **11** in THF solution at room temperature, as evidenced by an upfield-shifted resonance at $\delta(^{31}P) = -23$ ppm in the ^{31}P NMR and the disappearance of the C1–H proton resonance ($\delta(^1H) = 4.14$ ppm) in **10**[OTf]. Compound **11** gradually decomposes within several days under an inert atmosphere, but was isolated in high yield (86%) by extraction with Et_2O and fully characterized. Orange-colored crystals suitable for scXRD analysis were obtained by vapor diffusion of *n*-pentane into a saturated Et_2O solution and verified the assignment (**Figure 4b**). Relative to the parent structure, a prominent structural change is the formation of a strained four-membered ring, as evidenced by the remarkably shortened P1···N1 distance of 1.9670(11) Å. This distance lies between that of azaphosphetidines [2.170(3) Å] and their saturated analogues [1.7985(5) Å],[59,60] and is longer than that of reported amidophosphoranes [1.842(7) Å],[61] consistent with a strongly constrained interaction between nitrogen (N1) and phosphorus (P1) rather than a fully localized P–N single bond. The P1–C1 bond length is significantly shortened to 1.7488(12) Å, approaching the range observed for phosphonium-ylides.[62] In addition, the shortened C1–C2 bond [**10**[OTf], 1.490(5) Å; **11**, C1–C2 1.3987(17) Å] and the elongated C2–N1 bond [**10**[OTf], 1.298(5) Å; **11**, 1.3652(17) Å] indicate electron density transfer from N toward the central P-center.

Thus, the strong P/N interaction results in a rare strain-enforced bonding environment at the P atom.

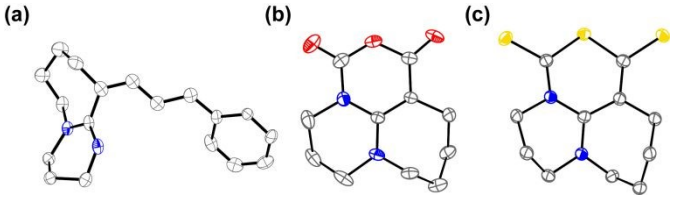

Figure 6 Molecular structures of *Z*,*E*-**17**$^+$ in *Z*,*E*-**17**[OTf] (**a**), **18** (**b**), and **20** (**c**). Hydrogen atoms, anions, and solvent molecules are omitted for clarity; thermal ellipsoids are displayed at 50% probability (100 K).

In analogy to conventional *Wittig* ylides, **11** exhibited canonical *Wittig*-type reactivity toward carbonyl electrophiles.[49,63–65] Reaction with paraformaldehyde and various substituted benzaldehydes afforded the corresponding DBU-derived products, isolated as their protonated triflate salts after work-up in good yields (**Figure 6a**, *Z*,*E*-**17**[OTf]; for **14**-**17**[OTf], see the **SI** for details). The phosphole oxide by-product **12** was isolated and characterized as a mixture of two diastereomers. Their diastereomeric configurations are differentiated by the relative orientation of the α-proton and the oxygen atom on the five-membered ring, as confirmed by scXRD analysis (see the **SI**, **Figure S94**).

Beyond its canonical *Wittig*-type behavior, compound **11** exhibited distinctive reactivity toward CO_2 (**Scheme 4)**. In an initial attempt, a C_6D_6 solution of **11** in a J. Young NMR tube was frozen in liquid nitrogen, evacuated, and charged with 2 bar CO_2. During thawing, an immediate color change from orange to pale yellow was observed, and the ^{31}P NMR spectrum confirmed the formation of **12**. Alongside **12**, the main product of this conversion was identified as oxazinedione derivative **18** by scXRD (**Figure 6b**) and was isolated as an air- and moisture-stable white solid. Remarkably, this transformation also proceeded efficiently at room temperature under 1 atm CO_2 (**Scheme 4**, **II**).

Similarly, CS_2 can also be activated in this manner. The reaction can proceed rapidly even at –78 °C, affording the phosphole sulfide **19** and the thiazinedithione derivative **20**, a heavier chalcogenide analogue of **18** featuring a C_2S_3 fragment (**Figure 5c**). Both species are air-stable and can be conveniently separated by extraction with toluene (52% for **20**).

Phosphorus ylides have shown potential for CO_2 transformation by forming zwitterionic intermediates with CO_2, which can undergo further reactions (including hydrolysis) to furnish carboxylic acid derivatives.[66,67] Interestingly, in our case, the endocyclic N atom participates in the formation of oxazinedione derivative **18**, consistent with a concerted bimolecular pathway rather than simple CO_2 adduct formation. Bimolecular CO_2 activation has only been rarely reported, typically in metal-mediated systems,[68] whereas more recent studies have mainly described the formation of CO_2 adducts.[61,66,69–71]

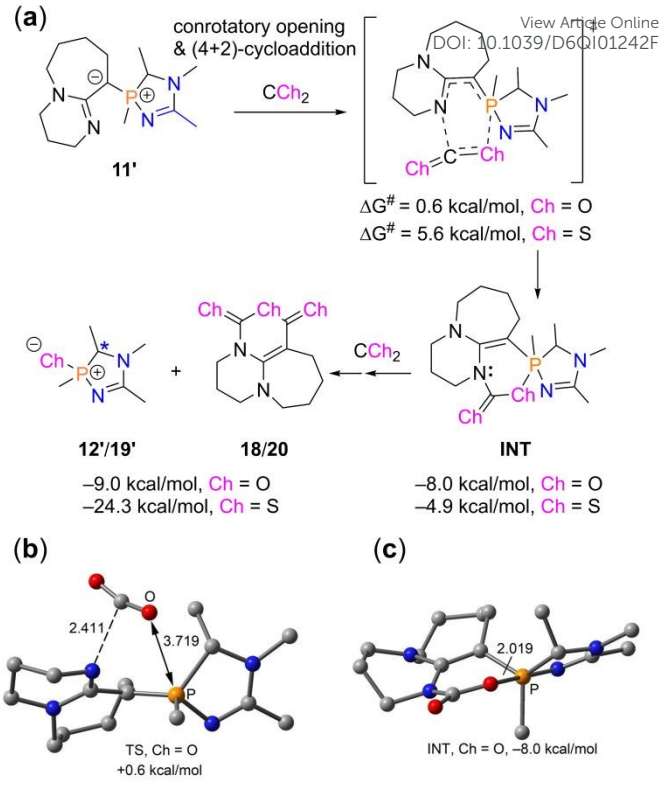

Figure 7 (**a**) Gibbs energies for the conversion of **11'** with CO_2 and CS_2 to yield products **12'**/**18** and **19'**/**20**. (**b**) BP86-D4/def2-TZVP geometries of the transition states for the (4+2) cycloaddition of **11'** with CO_2. (**c**) The resulting intermediates (**INT**) for CO_2. Distances in Å. A truncated model for **11** was used for calculation.

In contrast, compound **11** operates *via* a rare activation mode, which was further investigated using DFT analysis. **Figure 7a** illustrates the proposed mechanism for the transformation of ylide **11** with two equivalents of CO_2 (an analogous mechanism can be formulated for CS_2) (see detailed mechanism in **Figure S118**). For computational economy, we replaced the phenyl groups by methyl groups in compound **11** (denoted as **11'**). The process starts with the opening of the four-membered ring *via* a conrotatory reaction as has been studied previously in the literature.[72] This transient intermediate is immediately trapped by the CO_2 *via* a (4+2) cycloaddition reaction, forming a six-membered ring. The nucleophilic C-atom of the enamine-like unit attacks a second molecule of CO_2, forming a zwitterionic intermediate.

Then the anhydride functional group is formed upon the attack of the carboxylate oxygen atom to the "phosphaneyl-carbamate" fragment, eliminating compound **12'** and regenerating the enamine group to furnish **18**. The mechanism was analyzed from a thermodynamic point of view and by computing the transition state for the conrotatory opening of the four-membered ring in order to explain the activation process. The results are gathered in **Figure 7b**, evidencing that the first step is basically barrierless (0.6 kcal/mol) for CO_2 and proceeds with a low barrier (5.6 kcal/mol) for CS_2, which is consistent with the experimentally observed fast reaction and its occurrence at low temperature. This first mechanistic step is more exergonic for CO_2 than for CS_2 (–8.0 and –4.9 kcal/mol,

respectively), further supporting that this initial step is significantly more favored for CO_2.[73] The following addition of the second molecule of CO_2/CS_2 and elimination of the phosphole (sulfur/oxygen) chalcogenides **12'/19'** is also exergonic for both compounds, but in this case is more exergonic for CS_2 (−24.3 kcal/mol) than for CO_2 (−9.0 kcal/mol).

Conclusions

In summary, we have established a modular synthetic platform that converts readily accessible precursors into diverse cyclic phosphorus-containing frameworks. A practical three-component (1+2+2)-cycloaddition provides straightforward access to a series of diazaphospholium triflate salts. The imidazoliumyl (**L_C**) substituent serves as a programmable handle that directs subsequent, base-mediated diversification of these P(V) heterocycles. Treatment with DMAP triggers an unusual 1,2-phenyl migration, effecting a formal P(V)-to-P(III) conversion and furnishing cationic P(III)–DMAP adducts that can be further transformed into P-functionalized azaphospholes bearing P–C, P–O, and P–N bonds through reactions with appropriate nucleophiles. Together, these findings reveal a rare, operationally simple strategy for converting azaphospholium P(V) salts into isolable P(III) synthons. In contrast, treatment with DBU affords a DBU-derived phosphonium salt that can be deprotonated to an ylide. This *Wittig*-type species retains canonical olefination reactivity towards aldehydes while also enabling an atypical bimolecular activation of CO_2 and CS_2, leading to oxazinedione-type or thiazinedithione products alongside the corresponding phosphole chalcogenides. Ongoing work in our group aims to expand the (1+2+2)-cycloaddition to other dipolar two-atom components and nitrile classes, and to explore the coordination chemistry and catalytic utility of these new azaphosphole derivatives.

Author contributions

L. H., K. S., and J. J. W. conceptualized the study; L. H. conducted the experiments and optimized the syntheses, isolations, and purifications; R. G. and A. F. were responsible for mechanistic studies; J. F., P. R., and J. J. W. were responsible for X-ray data collection and refinement; K. S. and J. J. W. conceived, oversaw, and directed the project; L. H. wrote the initial draft of the paper. All authors contributed to data analysis, manuscript review and editing, and discussion.

Conflicts of interest

There are no conflicts to declare.

Data availability

The data supporting this article have been included in the main manuscript and the Electronic Supplementary Information (ESI). Crystallographic data have been deposited at the CCDC under deposition numbers 2543129–2543151.

View Article Online DOI: 10.1039/D6QI01242F

Acknowledgements

This work was supported by the German Research Foundation (DFG; WE 4621/6–1, WE 4621/6-2). L. H. was supported by the China Scholarship Council (CSC No. 202106360039). A. F. and R. G. M. thank MICIU/AEI (Spain) for financial support, project PID2023-148453NB-I00, co-funded by FEDER funds. We also thank Technische Universität Dresden (TUD) for support.

Notes and references

1 X. Chen, D. J. Kopecky, J. Mihalic, S. Jeffries, X. Min, J. Heath, J. Deignan, S. Lai, Z. Fu, C. Guimaraes, S. Shen, S. Li, S. Johnstone, S. Thibault, H. Xu, M. Cardozo, W. Shen, N. Walker, F. Kayser and Z. Wang, Structure-guided design, synthesis, and evaluation of guanine-derived inhibitors of the eIF4E mRNA-cap interaction, *J. Med. Chem.*, 2012, **55**, 3837–3851.

2 F.-R. Alexandre, A. Amador, S. Bot, C. Caillet, T. Convard, J. Jakubik, C. Musiu, B. Poddesu, L. Vargiu, M. Liuzzi, A. Roland, M. Seifer, D. Standring, R. Storer and C. B. Dousson, Synthesis and biological evaluation of aryl-phospho-indole as novel HIV-1 non-nucleoside reverse transcriptase inhibitors, *J. Med. Chem.*, 2011, **54**, 392–395.

3 M. F, The organic chemistry of phospholes, *Chem. Rev.*, 1988, **88**, 429–453.

4 M. P. Duffy, W. Delaunay, P.-A. Bouit and M. Hissler, π-Conjugated phospholes and their incorporation into devices: components with a great deal of potential, *Chem. Soc. Rev.*, 2016, **45**, 5296–5310.

5 W. Tang and X. Zhang, New chiral phosphorus ligands for enantioselective hydrogenation, *Chem. Rev.*, 2003, **103**, 3029–3070.

6 H. Fernández-Pérez, P. Etayo, A. Panossian and A. Vidal-Ferran, Phosphine-phosphinite and phosphine-phosphite ligands: preparation and applications in asymmetric catalysis, *Chem. Rev.*, 2011, **111**, 2119–2176.

7 Shu Kobayashi, Karl Anker Jorgensen, ed., *Cycloaddition reactions in organic synthesis*, Wiley-VCH, Weinheim, Germany, 2002.

8 L. Dettling, M. Papke, J. A. W. Sklorz, D. Buzsáki, Z. Kelemen, M. Weber, L. Nyulászi and C. Müller, A new access to diazaphospholes via cycloaddition-cycloreversion reactions on triazaphospholes, *Chem. Commun.*, 2022, **58**, 7745–7748.

9 Steffen Weidner, Jens Renner, Uwe Bergsträßer, Manfred Regitz*, Heinrich Heydt*, Organophosphorus Compounds, Part 168;1 1,3-Dipolar Cycloaddition Reactions of 1,3,5-Triphosphinines with Nitrile Oxides, *Synthesis*, 2004, 241–248.

10 J. A. W. Sklorz, S. Hoof, N. Rades, N. de Rycke, L. Könczöl, D. Szieberth, M. Weber, J. Wiecko, L. Nyulászi, M. Hissler and C. Müller, Pyridyl-functionalised 3H-1,2,3,4-triazaphospholes: synthesis, coordination chemistry and photophysical properties of low-coordinate phosphorus compounds, *Chem. Eur. J.*, 2015, **21**, 11096–11109.

11 S. L. Choong, A. Nafady, A. Stasch, A. M. Bond and C. Jones, The facile assembly of bis-, tris- and poly(triazaphosphole) systems using "click" chemistry, *Dalton Trans.*, 2013, **42**, 7775–7780.

12 A. H. Cowley, R. A. Kemp, J. G. Lasch, N. C. Norman and C. A. Stewart, Reaction of phosphenium ions with 1,3-dienes: a rapid synthesis of phosphorus-containing five-membered rings, *J. Am. Chem. Soc.*, 1983, **105**, 7444–7445.

13 R. J. Boyd, N. Burford and C. L. B. Macdonald, Ab Initio Studies of the Contrasting Butadiene Cheletropic and Diels−Alder Cycloaddition Reactivities Observed for "Carbenic" Phosphorus (Phosphenium) and Arsenic (Arsenium) Cations, *Organometallics*, 1998, **17**, 4014–4029.

14 M. B. Abrams, B. L. Scott and R. T. Baker, Sterically Tunable Phosphenium Cations: Synthesis and Characterization of Bis(arylamino)phosphenium Ions, Phosphinophosphenium Adducts, and the First Well-Defined Rhodium Phosphenium Complexes, *Organometallics*, 2000, **19**, 4944–4956.

15 N. Burford, P. J. Ragogna, R. McDonald and M. J. Ferguson, Phosphine Coordination Complexes of the Diphenylphosphenium Cation: A Versatile Synthetic Methodology for P−P Bond Formation, *J. Am. Chem. Soc.*, 2003, **125**, 14404–14410.

16 C. A. Caputo, J. T. Price, M. C. Jennings, R. McDonald and N. D. Jones, N-heterocyclic phosphenium cations: syntheses and cycloaddition reactions, *Dalton Trans.*, 2008, 3461–3469.

17 A. H. Cowley and R. A. Kemp, Synthesis and reaction chemistry of stable two-coordinate phosphorus cations (phosphenium ions), *Chem. Rev.*, 1985, **85**, 367–382.

18 N. Đorđević, R. Ganguly, M. Petković and D. Vidović, E-H (E = B, Si, C) Bond Activation by Tuning Structural and Electronic Properties of Phosphenium Cations, *Inorg. Chem.*, 2017, **56**, 14671–14681.

19 N. Đorđević, M. Q. Y. Tay, S. Muthaiah, R. Ganguly, D. Dimić and D. Vidović, C-F bond activation by transient phosphenium dications, *Inorg. Chem.*, 2015, **54**, 4180–4182.

20 B. D. Ellis, P. J. Ragogna and C. L. B. Macdonald, Computational insights into the acceptor chemistry of phosphenium cations, *Inorg. Chem.*, 2004, **43**, 7857–7867.

21 C. Hering, A. Schulz and A. Villinger, On the synthesis and reactivity of highly labile pseudohalogen phosphenium ions, *Inorg. Chem.*, 2013, **52**, 5214–5225.

22 A. Jayaraman, S. Nilewar, T. V. Jacob and B. T. Sterenberg, Sequential Electrophilic Substitution Reactions of Tungsten-Coordinated Phosphenium Ions and Phosphine Triflates, *ACS Omega*, 2017, **2**, 7849–7861.

23 Á. Kozma, T. Deden, J. Carreras, C. Wille, J. Petuškova, J. Rust and M. Alcarazo, Coordination Chemistry of Cyclopropenylidene-Stabilized Phosphenium Cations: Synthesis and Reactivity of Pd and Pt Complexes, *Chem. Eur. J.*, 2014, **20**, 2208–2214.

24 L. L. Liu, D. A. Ruiz, F. Dahcheh and G. Bertrand, Isolation of a Lewis base stabilized parent phosphenium (PH_2^+) and related species, *Chem. Commun.*, 2015, **51**, 12732–12735.

25 V. Nesterov, D. Reiter, P. Bag, P. Frisch, R. Holzner, A. Porzelt and S. Inoue, NHCs in Main Group Chemistry, *Chem. Rev.*, 2018, **118**, 9678–9842.

26 M. Olaru, D. Duvinage, E. Lork, S. Mebs and J. Beckmann, Transient Phosphenium and Arsenium Ions versus Stable Stibenium and Bismuthenium Ions, *Chem. Eur. J.*, 2019, **25**, 14758–14761.

27 M. Olaru, A. Mischin, L. A. Malaspina, S. Mebs and J. Beckmann, The Bis(ferrocenyl)phosphenium Ion Revisited, *Angew. Chem. Int. Ed.*, 2020, **59**, 1581–1584.

28 J. Petuškova, H. Bruns and M. Alcarazo, Cyclopropenylylidene-Stabilized Diaryl and Dialkyl Phosphenium Cations: Applications in Homogeneous Gold Catalysis, *Angew. Chem. Int. Ed.*, 2011, **50**, 3799–3802.

29 M. A. Samsonov, J. Vrána, P. Švec, V. Němec, E. Procházková, J. Cvačka and A. Růžička, Enhanced Reactivity of N-heterocyclic Halophosphines and Phosphenium Cations: The Activation of Carbon–Heteroatom and Boron–Heteroatom Bonds, *Chem. Eur. J.*, 2025, **31**, 2-8.

30 G. A. Seisenbaeva, V. G. Kessler, R. Pazik and W. Strek, N-Heterocyclic phosphenium cations: syntheses and cycloaddition reactions, *Dalton Trans.*, 2008, 3461–3469.

31 J. M. Slattery and S. Hussein, How Lewis acidic is your cation? Putting phosphenium ions on the fluoride ion affinity scale, *Dalton Trans.*, 2012, **41**, 1808–1815.

32 C. K. SooHoo and S. G. Baxter, Phosphenium ions as dienophiles, *J. Am. Chem. Soc.*, 1983, **105**, 7443–7444.

33 Steven A. Weissman, S. G. Baxter, Evidence For The Rearrangement Of P-Chloro-Phosphirenium Ions To P-Vinyl-Phosphenium Ions, *Tetrahedron Lett*, 1990, **31**, 819–822.

34 C. Stoian, N. Schmidt, T. J. Kuczmera, P. Puylaert, E. Lork, B. J. Nachtsheim, E. Hupf and J. Beckmann, Oxidative addition of diaryldichalcogenides to the diferrocenylphosphenium ion: synthesis, structure and organocatalytic activity, *Chem. Commun.*, 2025, **61**, 8256–8259.

35 M. Q. Y. Tay, G. Ilić, U. Werner-Zwanziger, Y. Lu, R. Ganguly, L. Ricard, G. Frison, D. Carmichael and D. Vidović, Preparation, Structural Analysis, and Reactivity Studies of Phosphenium Dications, *Organometallics*, 2016, **35**, 439–449.

36 R. Yadav, A. Sharma, B. Das, C. Majumder, A. Das, S. Sen and S. Kundu, Air and Water Stable Bicyclic (Alkyl)(Amino)Carbene Stabilized Phosphenium Cation: Reactivity and Selective Fluoride Ion Affinity, *Chem. Eur. J.*, 2024, **30**, e202401730.

37 Y. Unoh, K. Hirano and M. Miura, Metal-Free Electrophilic Phosphination/Cyclization of Alkynes, *J. Am. Chem. Soc.*, 2017, **139**, 6106–6109.

38 A. Jayaraman and B. T. Sterenberg, Phosphorus−Carbon Bond Forming Reactions of Diphenylphosphenium and Diphenylphosphine Triflate Complexes of Tungsten, *Organometallics*, 2016, **35**, 2367–2377.

39 D. Gasperini, S. E. Neale, M. F. Mahon, S. A. Macgregor and R. L. Webster, Phosphirenium Ions as Masked Phosphenium Catalysts: Mechanistic Evaluation and Application in Synthesis, *ACS Catal.*, 2021, **11**, 5452–5462.

40 L. You, D. Roth and L. Greb, Structural constraint at a P-P bond: phosphinophosphination of alkenes, alkynes, and carbonyls by a concerted mechanism, *Chem. Sci.*, 2025, **16**, 1716–1721.

41 A. Dumitrescu, H. Gornitzka, W. W. Schoeller, D. Bourissou and G. Bertrand, A Crystalline Phosphenium Salt Featuring the Electron-Withdrawing 2,6-Bis(trifluoromethyl)phenyl Group, *Eur. J. Inorg. Chem.*, 2002, **2002**, 1953–1956.

42 J. Fidelius, K. Schwedtmann, S. Schellhammer, J. Haberstroh, S. Schulz, R. Huang, M. C. Klotzsche, A. Bauzá, A. Frontera, S. Reineke and J. J. Weigand, Convenient access to π-conjugated 1,3-azaphospholes from alkynes via [3+2]-cycloaddition and reductive aromatization, *Chem*, 2024, **10**, 644–659.

43 J. Fidelius, K. Schwedtmann, S. Schellhammer, R. Huang, F. Hennersdorf, M. Fink, J. Haberstroh, A. Bauzá, A. Frontera, S. Reineke and J. J. Weigand, 1,3-Dipolar cycloaddition reactions of triflatophosphanes to afford functionalized azaphospholium salts and azaphospholes, *Inorg. Chem. Front.*, 2025, **12**, 3324–3333.

44 P. Royla, K. Schwedtmann, Z. Han, J. Fidelius, D. P. Gates, R. M. Gomila, A. Frontera and J. J. Weigand, Cationic Phosphinidene as a Versatile P_1 Building Block: L_C-P+ Transfer from Phosphonio-Phosphanides $[L_C\text{-}P\text{-}PR_3]^+$ and Subsequent LC Replacement Reactions (L_C = N-Heterocyclic Carbene), *J. Am. Chem. Soc.*, 2023, **145**, 10364–10375.

45 J. J. Weigand, K.-O. Feldmann and F. D. Henne, Carbene-stabilized phosphorus(III)-centered cations $[LPX_2]^+$ and $[L_2PX]^{2+}$ (L = NHC; X = Cl, CN, N_3), *J. Am. Chem. Soc.*, 2010, **132**, 16321–16323.

46 Anca Dumitrescu, Heinz Gornitzka, Wolfgang W. Schoeller, Didier Bourissou, Guy Bertrand, A Crystalline Phosphenium Salt Featuring the Electron-Withdrawing 2,6-Bis(trifluoromethyl)phenyl Group, *Eur. J. Inorg. Chem.*, 2002, 1953–1956.

47 R. M. Tipker, J. A. Muldoon, D. H. Pham, B. R. Varga, R. P. Hughes, D. S. Glueck, G. J. Balaich and A. L. Rheingold, Configurational Lability at Tetrahedral Phosphorus: syn/anti -Isomerization of a P-Stereogenic Phosphiranium Cation by Intramolecular Epimerization at Phosphorus, *Angew. Chem. Int. Ed.*, 2022, **61**, e202110753.

48 S. Fankel, H. Helten, G. von Frantzius, G. Schnakenburg, J. Daniels, V. Chu, C. Müller and R. Streubel, Novel access to azaphosphiridine complexes and first applications using Brønsted acid-induced ring expansion reactions, *Dalton Trans.*, 2010, **39**, 3472–3481.

49 G. Wittig, From diyls to ylides to my idyll, *Science*, 1980, **210**, 600–604.

View Article Online
DOI: 10.1039/D6QI01242F

50 D. Lednicer, Preparation of 1,6-diarylhexatrienes by a modified Wittig reaction, *J. Org. Chem.*, 1971, **36**, 3473–3474.

51 Y. Masuda, D. Ikeshita, K. Higashida, M. Yoshida, N. Ishida, M. Murakami and M. Sawamura, Photocatalytic 1,2-Phosphorus-Migrative [3 + 2] Cycloaddition of Tri(*t*-butyl)phosphine with Terminal Alkynes, *J. Am. Chem. Soc.*, 2023, **145**, 19060–19066.

52 N. Burford, P. Losier, A. D. Phillips, P. J. Ragogna and T. S. Cameron, Nitrogen ligands on phosphorus(III) Lewis acceptors: A versatile new synthetic approach to unusual N-P structural arrangements, *Inorg. Chem.*, 2003, **42**, 1087–1091.

53 M. Donath, K. Schwedtmann, T. Schneider, F. Hennersdorf, A. Bauzá, A. Frontera and J. J. Weigand, Direct conversion of white phosphorus to versatile phosphorus transfer reagents via oxidative onioation, *Nat. Chem.*, 2022, **14**, 384–391.

54 F. Mathey, The organic chemistry of phospholes, *Chem. Rev.*, 1988, **88**, 429–453.

55 A. Kers, I. Kers and J. Stawinski, The reaction of diphenyl and dialkyl phosphorochloridates with 1,8-diazabicyclo[5.4.0]undec-7-ene (DBU). Formation of phosphonate diesters via N→C phosphorus migration, *J. Chem. Soc., Perkin Trans. 2*, 1999, 2071–2075.

56 M. O'Reilly, R. Pattacini and P. Braunstein, Anion effect in the diastereoselective formation of bischelated Ni(II) complexes with a novel, chiral phosphine derived from 1,8-diazabicyclo5.4.0undec-7-ene (DBU), *Dalton Trans.*, 2009, 6092–6095.

57 P. Pyykkö and M. Atsumi, Molecular single-bond covalent radii for elements 1-118, *Chem. Eur. J.*, 2009, **15**, 186–197.

58 M. Mantina, A. C. Chamberlin, R. Valero, C. J. Cramer and D. G. Truhlar, Consistent van der Waals radii for the whole main group, *J. Phys. Chem. A*, 2009, **113**, 5806–5812.

59 T. Kawashima, T. Soda and R. Okazaki, Synthesis, Structure, and Thermolysis of N-Apical 1,2λ^5-Azaphosphetidines with a Pentacoordinate P Center and the First Observation of Their N-Equatorial Pseudorotamers, *Angew. Chem. Int. Ed.*, 1996, **35**, 1096.

60 N. Kano, A. Kikuchi and T. Kawashima, The first isolable pentacoordinate 1,2 lambda 5-azaphosphetine: synthesis, X-ray crystallographic analysis, and dynamic behaviour, *Chem. Commun.*, 2001, 2096–2097.

61 L. J. Hounjet, C. B. Caputo and D. W. Stephan, Phosphorus as a Lewis acid: CO_2 sequestration with amidophosphoranes, *Angew. Chem. Int. Ed.*, 2012, **51**, 4714–4717.

62 J. C. J. Bart, Structure of the non-stabilized phosphonium ylid methylenetriphenylphosphorane, *J. Chem. Soc., B*, 1969, 350–365.

63 Bruce E. Maryanoff, Allen B. Reitz, The Wittig olefination reaction and modifications involving phosphoryl-stabilized carbanions. Stereochemistry, mechanism, and selected synthetic aspects, *Chem. Rev.*, 1989, 863–927.

View Article Online
DOI: 10.1039/D6QI01242F

64 Edwin Vedejs, C. F. Marth, Mechanism of Wittig reaction: evidence against betaine intermediates, *J. Am. Chem. Soc.*, 1990, 3905–3909.

65 P. A. Byrne and D. G. Gilheany, The modern interpretation of the Wittig reaction mechanism, *Chem. Soc. Rev.*, 2013, **42**, 6670–6696.

66 H. Zhou, G.-X. Wang, W.-Z. Zhang and X.-B. Lu, CO_2 Adducts of Phosphorus Ylides: Highly Active Organocatalysts for Carbon Dioxide Transformation, *ACS Catal.*, 2015, **5**, 6773–6779.

67 H. J. Bestmann, T. Denzel and H. Salbaum, Reaktion von phosphinalkylenen mit CO_2. Eine neue möglichkeit zur synthese von carbonsäuren, allenen und acylyliden, *Tetrahedron Lett*, 1974, **15**, 1276–1974.

68 J. Langer, A. Hamza and I. Pápai, RuBisCO-Inspired CO_2 Activation and Transformation by an Iridium(I) Complex, *Angew. Chem. Int. Ed.*, 2018, **57**, 2455–2458.

69 D. W. Stephan, Frustrated Lewis pairs: from concept to catalysis, *Acc. Chem. Res.*, 2015, **48**, 306–316.

70 D. W. Stephan and G. Erker, Frustrated Lewis pair chemistry: development and perspectives, *Angew. Chem. Int. Ed.*, 2015, **54**, 6400–6441.

71 C.-X. Guo, K. Schwedtmann, J. Fidelius, F. Hennersdorf, A. Dickschat, A. Bauzá, A. Frontera and J. J. Weigand, Bifunctional Fluorophosphonium Triflates as Intramolecular Frustrated Lewis Pairs: Reversible CO_2 Sequestration and Binding of Carbonyls, Nitriles and Acetylenes, *Chem. Eur. J.*, 2021, **27**, 13709–13714.

72 Z. Mucsi, I. Hermecz, B. Viskolcz, I. G. Csizmadia and G. Keglevich, The influence of exocyclic phosphorous substituents on the intrinsic stability of four-membered heterophosphetes: a theoretical study, *Tetrahedron*, 2008, **64**, 1868–1878.

73 K. An and J. Zhu, Why Does Activation of the Weaker C═S Bond in CS_2 by P/N-Based Frustrated Lewis Pairs Require More Energy Than That of the C═O Bond in CO_2? A DFT Study, *Organometallics*, 2014, **33**, 7141–7146.

View Article Online
DOI: 10.1039/D6QI01242F

Data availability. The data supporting the findings of this study, including CIF files, NMR spectra, and computational details, are available in the ESI. Additional data can be obtained from the corresponding author upon reasonable request. CCDC Deposition numbers 2543129–2543151 contain the supplementary crystallographic data for this paper. These data are provided free of charge by the joint Cambridge Crystallographic Data Centre and Fachinformationszentrum Karlsruhe Access Structures service (https://www.ccdc.cam.ac.uk/).